





Coastal macroalgae aquaculture reduces carbon dioxide emission in a subtropical enclosed bay: Insights from eddy covariance measurements

Yueting Deng^{a,b,c,d}, Xianghui Guo^{a,c,e}, Xiaosong Zhao^f, Haitao Zhou^g , Lichun Li^h,
Yougan Chen^{e,i}, Xudong Zhu^{a,b,c,d,i,*} 

^a State Key Laboratory of Marine Environmental Science, Xiamen University, Xiamen, Fujian, China

^b Key Laboratory of the Coastal and Wetland Ecosystems (Ministry of Education), Xiamen University, Xiamen, Fujian, China

^c National Observation and Research Station for the Taiwan Strait Marine Ecosystem (Xiamen University), Zhangzhou, Fujian, China

^d College of the Environment and Ecology, Xiamen University, Xiamen, Fujian, China

^e College of Ocean and Earth Sciences, Xiamen University, Xiamen, Fujian, China

^f Key Laboratory of Lake and Watershed Science for Water Security, Nanjing Institute of Geography and Limnology, Chinese Academy of Sciences, Nanjing, Jiangsu, China

^g Southern Marine Science and Engineering Guangdong Laboratory (Zhuhai), Zhuhai, Guangdong, China

^h Fujian Key Laboratory of Severe Weather, Fuzhou, Fujian, China

ⁱ Shenzhen Research Institute of Xiamen University, Shenzhen, Guangdong, China

ARTICLE INFO

Keywords:
Seaweed
Carbon flux
Eddy covariance
Sansha Bay

ABSTRACT

Macroalgae aquaculture has been increasingly recognized as a promising nature-based solution to enhance carbon sinks towards climate change mitigation. However, a limited understanding of the temporal patterns of air-sea carbon dioxide (CO₂) fluxes and their environmental controls across time scales poses an enormous obstacle to the carbon sink potential assessment of macroalgae aquaculture. Here, we utilized the eddy covariance (EC) approach to acquire continuous and high-frequency measurements of net ecosystem exchange (NEE) of CO₂ over the macroalgae aquaculture in a subtropical enclosed bay in southeast China, throughout one full year from April 2023 to March 2024. The results showed (a) this ecosystem acted as a CO₂ source in most months with the strongest source and sink occurring at the beginning of autumn and winter, respectively; (b) annually this ecosystem emitted 58.9 g C m⁻² of CO₂ into the atmosphere with nighttime source contributing 84.7 %; (c) macroalgae aquaculture of *Saccharina japonica* and *Gracilariopsis Lemaneiformis* tended to reduce CO₂ emission from this ecosystem, while the extent of the reduction varied with aquaculture types and growth stages; (d) temporal variability of NEE was most correlated with air temperature, while faster tidal currents tended to stimulate CO₂ emission during both flood and ebb tides. The strong temporal variability of NEE highlights the importance of high-frequency EC measurements in improving the understanding of temporal patterns of air-sea CO₂ fluxes over the macroalgae aquaculture ecosystems. This study suggests that macroalgae aquaculture has the potential to mitigate CO₂ emission, although the ecosystem itself overall functions as a net CO₂ source on an annual time scale.

1. Introduction

In addition to direct human emission reductions, such as reducing the burning of fossil fuels, an important way to mitigate climate change is to enhance the carbon sink potential of natural ecosystems and thus promote atmospheric carbon dioxide (CO₂) removal (CDR). As one of the fastest-growing and most productive coastal ecosystems on the earth, the maximum net primary productivity of macroalgae (or

seaweed) even exceeds that of seagrasses, salt marshes, and mangroves combined (Krause-Jensen and Duarte, 2016; Duarte, 2017). More and more studies are now proving the carbon sink function of macroalgae (Krause-Jensen and Duarte, 2016; Ortega et al., 2019; Filbee-Dexter et al., 2023). Macroalgae aquaculture has been recognized as a promising nature-based solution to CDR due to its low cost and environmental co-benefits (Bach et al., 2021; Duarte et al., 2022; Gao et al., 2022).

Macroalgae absorb dissolved inorganic carbon (DIC) from seawater

* Corresponding author at: State Key Laboratory of Marine Environmental Science, Xiamen University, Xiamen, Fujian, China.

E-mail address: xdzhu@xmu.edu.cn (X. Zhu).

<https://doi.org/10.1016/j.agee.2025.109576>

Received 12 December 2024; Received in revised form 14 February 2025; Accepted 17 February 2025

0167-8809/© 2025 Elsevier B.V. All rights are reserved, including those for text and data mining, AI training, and similar technologies.

through photosynthesis of the thallus. The carbon released from the erosion and decay of macroalgae thallus enters the seawater environment in the form of dissolved or particulate organic carbon (Hurd et al., 2024). A portion of the released carbon is sequestered through burial in the sediment or transported to the deep sea for long-term storage (Ross et al., 2023; Hurd et al., 2024). Another portion is reconverted by microbial respiration or mineralization and emitted back into the atmosphere (Wada et al., 2008; Weigel et al., 2022). For example, the organic carbon released by macroalgae at the late growth stage stimulates microbial metabolism and thus converts the macroalgae aquaculture ecosystem from a sink to a source of atmospheric CO₂ (Xiong et al., 2024). Overall, the carbon dynamics in macroalgae involve several complex biotic and abiotic processes varying across spatial and temporal scales, making it difficult to accurately quantify the carbon budget (Hurd et al., 2022).

To date, most studies have focused on seawater particulate/dissolved organic carbon and sedimentary carbon to assess the CDR potential of macroalgae (Pan et al., 2019; Watanabe et al., 2020; Perkins et al., 2022; Li et al., 2022a). However, the direct CO₂ exchange between macroalgae ecosystems and the atmosphere has been less studied, leading to a critical knowledge gap that hinders the assessment of the carbon sink potential of macroalgae (Hurd et al., 2022). Direct flux measurements at the air-sea interface are not equivalent to the flux profiles within seawater. First, seawater surfaces at sites where carbon burial occurs do not necessarily absorb atmospheric CO₂ directly (Roth et al., 2023). Second, the water column that has reduced CO₂ in seawater as a result of macroalgae photosynthesis may move into new locations with tidal or current action and absorb atmospheric CO₂ outside the original habitat (Watanabe et al., 2020). In addition, as a result of lateral carbon inputs, even an autotrophic ecosystem may still be a net source of atmospheric CO₂ locally if the carbon remineralization from lateral inputs is high (Gallagher et al., 2022; Roth et al., 2023).

Therefore, continuous measurements of air-sea CO₂ fluxes are important for determining whether macroalgal ecosystems act as a net CO₂ sink or source. The eddy covariance (EC) approach can provide continuous and high-frequency measurements of CO₂ fluxes. However, the approach has been mainly applied to terrestrial ecosystems and coastal ecosystems such as mangroves and salt marshes (Zhu et al., 2024a, 2024b). The EC applications in global macroalgal ecosystems are very few, especially in macroalgae aquaculture (Ikawa and Oechele, 2015). In addition to the lack of understanding of the temporal variability of air-sea CO₂ fluxes over macroalgae ecosystems, the fluxes may also vary with different aquaculture types, stages, and management. In this context, the use of continuous and high-frequency measurements is of great significance to quantify the air-sea CO₂ fluxes over macroalgae aquaculture and to reveal their complex temporal heterogeneity.

Macroalgae aquaculture worldwide is growing at an annual rate of 6.4 % and is predicted to cover an area of 15,733 km² by 2050 (Duarte et al., 2022). Almost all of the global macroalgae aquaculture production comes from Asia, with China accounting for half of the global production. Currently, there is no such study to assess the temporal patterns of air-sea CO₂ fluxes across time scales over mariculture aquaculture based on EC flux measurements. In this study, we utilized the EC approach to acquire continuous and high-frequency measurements of net ecosystem exchange (NEE) over the macroalgae aquaculture in a subtropical enclosed bay (Sansha Bay) in southeast China, throughout one full year from April 2023 to March 2024. The two specific objectives of this study are (1) to examine the temporal variability of NEE and its environmental controls across various time scales and aquaculture activities, and (2) to assess the temporal pattern of the CO₂ source-sink of macroalgae ecosystem and its potential contribution from aquaculture activities.

2. Materials and methods

2.1. Study area

The study area is located in the macroalgae aquaculture area in Sansha Bay of southeast China, which is a semi-enclosed bay with a narrow gateway of only 3 km wide to the East China Sea (Fig. 1). This bay has a subtropical monsoonal climate with mean annual air and water temperatures of 20.3°C and 18.5°C, respectively, and a mean annual seawater salinity of 29.8 ppt (Wang et al., 2009). It experiences irregular semi-diurnal tides with a mean tidal range of 5.35 m and a higher ebb tide rate than the flood tide rate (Ye et al., 2007). The study area with macroalgae aquaculture is located in the northeastern inner bay without experiencing direct freshwater inputs from Jiaoxi river running into the northwest of the bay (Han et al., 2021a). There are two aquaculture types in the study area, i.e., raft aquaculture and cage aquaculture. Raft aquaculture is dominated by *Saccharina japonica* and *Gracilariopsis Lemaneiformis* and cage aquaculture is mainly for *Apostichopus japonicus*. For macroalgae aquaculture, the culture period of *S. japonica* is from December to May of the next year, while the culture period of *G. Lemaneiformis* is shorter but can be planted throughout most of the year.

2.2. Eddy covariance measurements

The EC system (26.7218°N, 119.9871°E; ChinaFLUX and USCCC), deployed ~5 m above the surface water of the macroalgae, consisted of an open-path gas analyzer of CO₂ (Li-7500, Li-COR Inc., Lincoln, NE, USA) and a three-axis sonic anemometer (CSAT-3, Campbell Scientific Inc., Logan, UT, USA) (Fig. 1b). To reduce potential swaying issue, the EC system was deployed on a tower platform fixed to a large fish raft used for *A. japonicus* cultivation. The footprint climatology analyses following Kormann and Meixner (2001) confirmed that 90 % of the fluxes were contributed from the aquaculture area within ~400 m around the tower (Fig. 1c). To ensure high quality of the flux data, regular instrument maintenance including cleaning the sensor mirror of gas analyzer were performed roughly every week. The raw 10-Hz data were processed into 30-min time-series data using the EddyPro software (Li-COR Inc.) with a series of flux corrections (including axis rotation, frequency response, ultrasonic, and WPL corrections) and quality control (including steady state, turbulent condition, statistical, and absolute limit tests) processes (Zhu et al., 2021). The 0–1–2 labeling system (Mauder et al., 2013) was applied to label the flux data quality, and the data with a quality flag of 2 were excluded from further analyses. Flux data under conditions of rainfall and insufficient nighttime turbulence were also excluded.

2.3. Ancillary measurements

The meteorological data, including solar radiation, wind speed/direction, air temperature (T_a), and rainfall, were measured by an integrated weather station (ATMOS 41, METER Group Inc., Pullman, WA, USA) deployed on the tower platform. Water quality parameters from a nearby buoy system included water temperature (T_w), dissolved oxygen (DO), and chlorophyll-a (Chl-a). T_w and DO were measured with a high-accuracy CTD sensor (SBE 37 SMP-ODO, Sea-bird, USA), while Chl-a was recorded by a fluorimeter (ECO FLS, WET Labs, USA). To match the EC data, all ancillary measurements were converted into 30-minute time series data. The percentage of DO (DO%) was also converted from DO (Benson and Krause, 1984) to consider the effect of water temperature fluctuations in assessing the photosynthetic effect of macroalgae. To map the spatio-temporal evolution of the macroalgae aquaculture, drone and satellite remote sensing imagery were combined to determine the main aquaculture types (Fig. S1). To examine the potential swaying issue on NEE, we also used one-month (December 2023) attitude data measured by a high-performance Attitude and Heading Reference

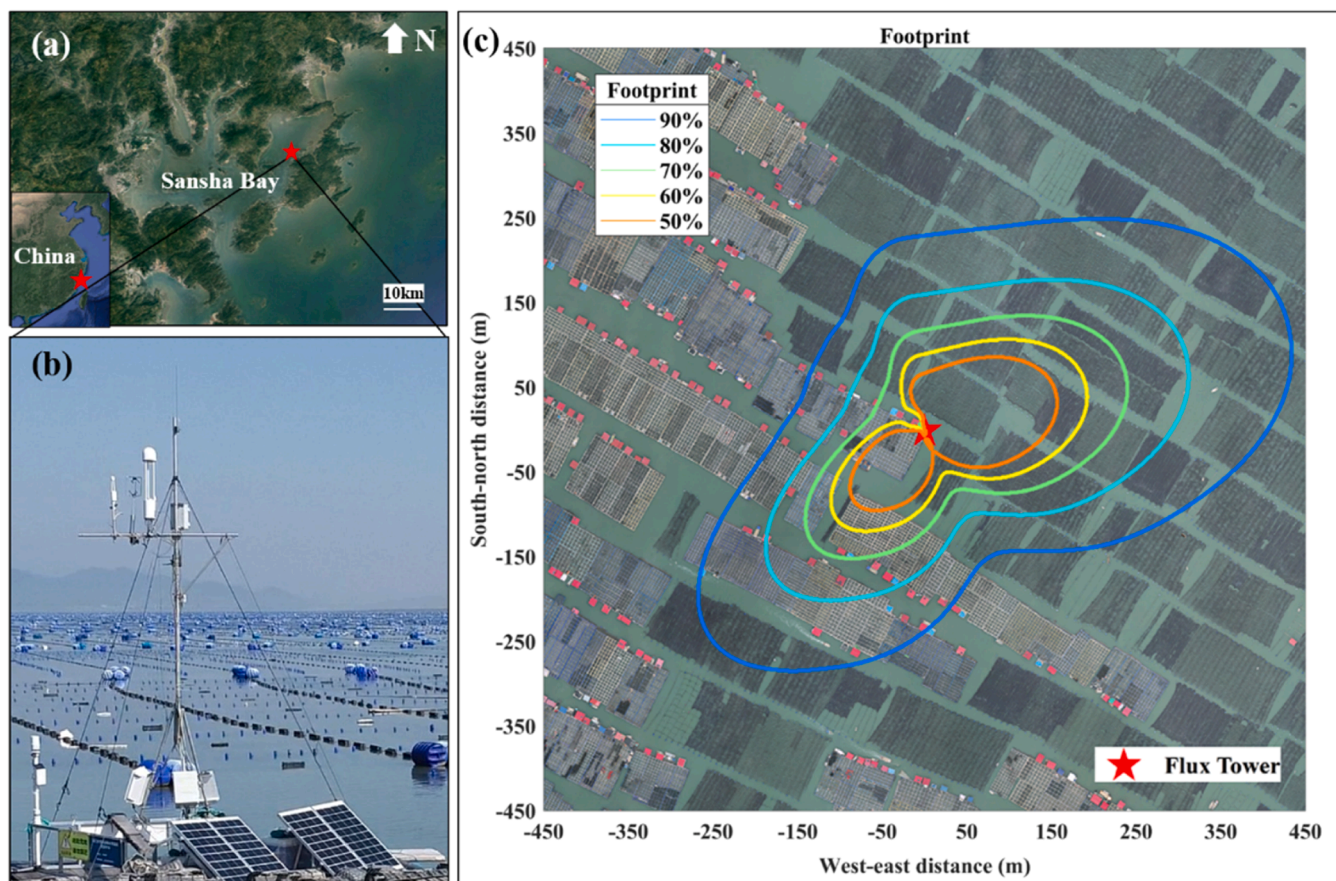


Fig. 1. Location of the study area within a subtropical enclosed bay in southeast China (Sansha Bay) (a), where an eddy covariance flux tower (b) was established over the macroalgae aquaculture in the northeastern inner bay shown with a drone image (acquired on January 26, 2024) overlaid by the flux footprint climatology (c).

System (AHRs) Ellipse-A (SBG system, France) attitude system to correct wind speeds and thus fluxes following Edson et al. (1998). The analyses revealed that the attitude-corrected flux results had only a 3 % relative deviation from the uncorrected original fluxes. To ensure consistency, all flux data analyses were based on the uncorrected original fluxes, due to the lack of concurrent attitude data over the one-year study period.

2.4. Statistical analyses

To reduce the bias in the aggregation due to unbalanced data availability between daytime and nighttime, we conducted quality control separately for daytime and nighttime data. Specifically, the days with valid daytime or nighttime 30-min records less than a quarter of the total number of records were excluded from the aggregation. Over the one-year study period, after excluding poor data due to quality issues and instrument failures, the percentages of valid 30-min and daily NEE data were 65.2 % and 93.4 %, respectively. Mean diurnal variations were used to analyze diurnal variation in NEE for each month and different culture periods/stages. To better analyze NEE among different culture periods/stages, we divided the one-year study period into the following periods according to the dominant culture activities: April and May 2023 and from December 2023 to March 2024 for *S. japonica* culture period (December and January for the rapid growth stage, February and March for the middle growth stage, and April and May for the harvesting stage); June, July, October, and November 2023 for *G. Lemaneiformis* culture period. August and September 2023 were treated as non-farming periods without macroalgae farming.

To compare the correlation between daily NEE data and environmental variables, Pearson's correlation coefficients calculated on a

pairwise basis were used to explore the potential impacts of various environmental factors on the daily CO₂ flux variations. To examine the tidal impacts on the response of NEE to environmental controls, we analyzed the data of 30-min NEE with varying tidal levels. Specifically, tidal levels were divided into six equal parts from low to high tide (1 H ~ 6 H) and then treated 1 H and 6 H as the "slow" group and 3 H and 4 H as the "fast" group (Fig. S2). For each of these two groups, the NEE data were binned by an environmental factor (20 percentile-based bins) to calculate the mean values and standard deviations, and then linear regressions were applied to fit the mean values. The difference in fitting lines between the "slow" and "fast" groups indicated the effect of tidal currents on the response of NEE. We also compared the mean values of NEE and wind speeds across all tidal levels (1 H ~ 6 H) for both daytime and nighttime. In this study, negative and positive values of gas flux indicated a sink (downward air-to-water flux) and a source (upward water-to-air flux), respectively. All data processing and statistical analyses were performed in MATLAB software (MathWorks Inc., Natick, MA, USA).

3. Results

3.1. Temporal variations in environmental factors

The daily variation of meteorological and water quality data observed over the year included radiation, wind speed, rainfall, Ta, Tw, DO and Chl-a (Fig. 2). The daily radiation had a strong fluctuation, varying from 3.1 MJ m⁻² day⁻¹ to 76.6 MJ m⁻² day⁻¹ (Fig. 2a). The annual average wind speed was 3.0 m s⁻¹ with higher mean daily wind speeds (up to 10.7 m s⁻¹) in September and October. Daily variations in

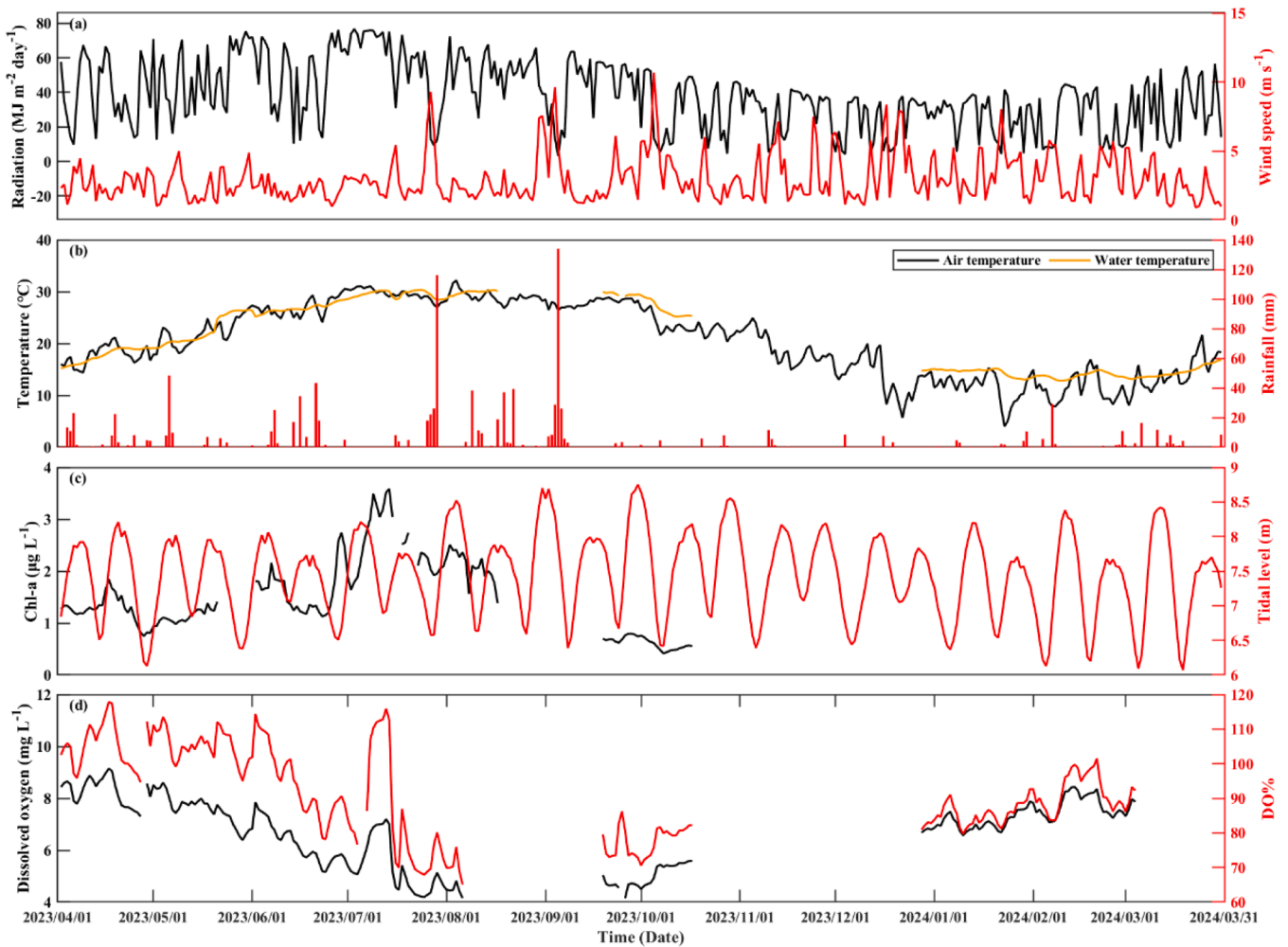


Fig. 2. Temporal variations in daily environmental factors from April 2023 to March 2024, including (a) cumulative radiation, mean wind speed, (b) mean air/water temperature, cumulative rainfall, (c) mean chlorophyll-a (Chl-a), maximum tidal level, (d) mean dissolved oxygen (DO) and mean DO%.

Ta ranged from 4.1°C to 32.2°C with a mean value of 20.5°C, while daily variations in Tw ranged from 12.8°C to 30.4°C with a mean value of 21.1°C (Fig. 2b). Daily mean Ta and Tw exhibited similar seasonal variations with the maximum and minimum values in August and January, respectively. During the study period, the maximum daily rainfall reached 134 mm with more rainfall occurring in summer. The daily variation of the maximum tidal height reflected the semi-diurnal tidal pattern, ranging from 6.1 m to 8.8 m (Fig. 2c). Chl-a and DO had strong daily variations with the average value of 1.5 $\mu\text{g L}^{-1}$ (0.4 ~ 3.6 $\mu\text{g L}^{-1}$) and 6.7 mg L^{-1} (3.8 ~ 9.1 mg L^{-1}), respectively (Figs. 2c and 2d). Daily DO% had a similar temporal variation with daily DO with an average daily DO% of 91.1 % (60.3 % ~ 117.8 %).

3.2. Temporal variations in CO₂ flux

Temporal variations in daily and monthly cumulative NEE were shown during the study period, along with daily variations in daytime and nighttime NEE (Fig. 3). During the daytime, daily NEE ranged from $-0.89 \text{ g C m}^{-2} \text{ day}^{-1}$ to $0.96 \text{ g C m}^{-2} \text{ day}^{-1}$ with a mean value of $0.03 \text{ g C m}^{-2} \text{ day}^{-1}$ (Fig. 3a). During the nighttime, daily NEE ranged from $-1.45 \text{ g C m}^{-2} \text{ day}^{-1}$ to $1.06 \text{ g C m}^{-2} \text{ day}^{-1}$ with a mean value of $0.14 \text{ g C m}^{-2} \text{ day}^{-1}$ (Fig. 3b). In terms of the whole day, daily NEE ranged from $-2.34 \text{ g C m}^{-2} \text{ day}^{-1}$ to $1.52 \text{ g C m}^{-2} \text{ day}^{-1}$ with a mean value of $0.16 \text{ g C m}^{-2} \text{ day}^{-1}$ (Fig. 3c). This ecosystem showed a weak source of CO₂ during the day and a strong source of CO₂ at night, resulting in an all-day source of CO₂. There was a similar variation in

monthly NEE between daytime and nighttime. Temporal variations in monthly NEE indicated that this ecosystem acted as a weak daytime CO₂ source and a strong nighttime CO₂ source for most of the year, while it acted as a CO₂ sink during November, December, and January (Fig. 3d). The ecosystem showed the strongest CO₂ source ($18.83 \text{ g C m}^{-2} \text{ month}^{-1}$) and sink ($-13.52 \text{ g C m}^{-2} \text{ month}^{-1}$) in August and December, respectively, with a mean monthly source of $5.04 \text{ g C m}^{-2} \text{ month}^{-1}$.

Mean diurnal variations in NEE showed large fluctuations and differed among months and seasons (Fig. 4): spring ($-0.38 \sim 0.60 \mu\text{mol m}^{-2} \text{ s}^{-1}$), summer ($-0.45 \sim 1.10 \mu\text{mol m}^{-2} \text{ s}^{-1}$), autumn ($-0.41 \sim 0.59 \mu\text{mol m}^{-2} \text{ s}^{-1}$), and winter ($-0.55 \sim 0.30 \mu\text{mol m}^{-2} \text{ s}^{-1}$). During the daytime, spring ($0.10 \pm 0.18 \mu\text{mol m}^{-2} \text{ s}^{-1}$) and summer ($0.02 \pm 0.23 \mu\text{mol m}^{-2} \text{ s}^{-1}$) overall acted as a CO₂ source, while autumn ($-0.03 \pm 0.21 \mu\text{mol m}^{-2} \text{ s}^{-1}$) and winter ($-0.08 \pm 0.17 \mu\text{mol m}^{-2} \text{ s}^{-1}$) overall acted as a CO₂ sink. At night, only winter was a sink of CO₂ ($-0.20 \pm 0.16 \mu\text{mol m}^{-2} \text{ s}^{-1}$), while all other seasons were sources of CO₂: spring ($0.32 \pm 0.13 \mu\text{mol m}^{-2} \text{ s}^{-1}$), summer ($0.71 \pm 0.32 \mu\text{mol m}^{-2} \text{ s}^{-1}$), and autumn ($0.24 \pm 0.19 \mu\text{mol m}^{-2} \text{ s}^{-1}$). On the monthly scale, summer showed stronger flux variability than other seasons, and the strongest flux variability occurred in August with a diurnal difference of $2.43 \mu\text{mol m}^{-2} \text{ s}^{-1}$ ($-0.52 \sim 1.91 \mu\text{mol m}^{-2} \text{ s}^{-1}$) (Fig. 4h). The smallest flux variability occurred in April, with a diurnal difference of $0.93 \mu\text{mol m}^{-2} \text{ s}^{-1}$ ($-0.37 \sim 0.56 \mu\text{mol m}^{-2} \text{ s}^{-1}$) (Fig. 4c).

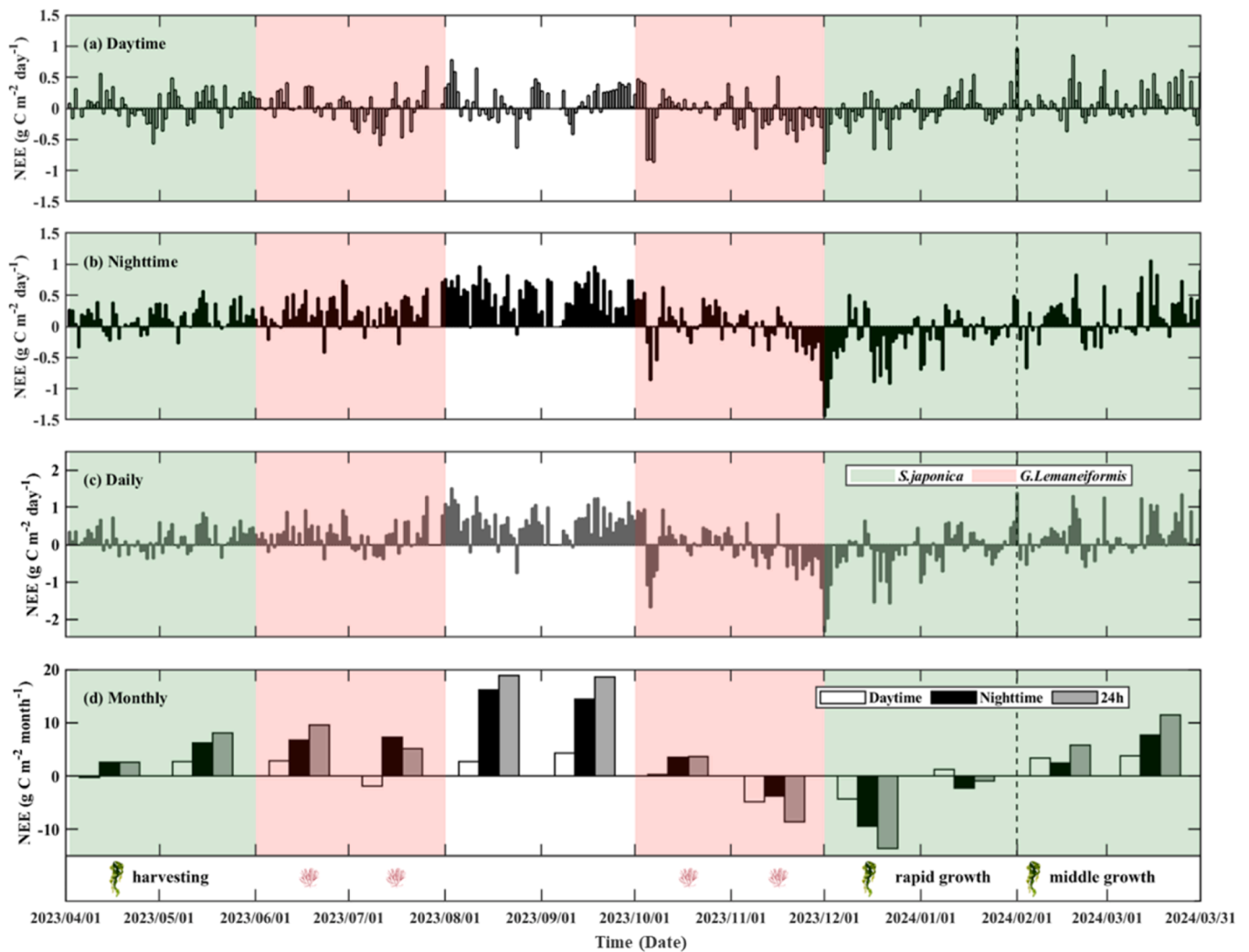


Fig. 3. Temporal variations in daytime (a), nighttime (b), daily (c), and monthly (d) cumulative net ecosystem exchange (NEE) over the macroalgae aquaculture from April 2023 to March 2024. Monthly cumulative NEE are shown for daytime, nighttime, and 24-hour periods. Macroalgae farming periods of *S. japonica* (April and May of 2023 and December 2023 ~ March 2024) and *G. Lemaneiformis* (June, July, October, and November of 2023) are indicated with green and red shades, respectively. The half-year farming period of *S. japonica* can be further divided into three two-month stages including rapid growth, middle growth, and harvesting.

3.3. CO₂ flux during different farming periods

The diurnal pattern of NEE during different farming periods varied greatly (Fig. 5). The *S. japonica* farming period acted as a weak CO₂ source both during the daytime ($0.004 \mu\text{mol m}^{-2} \text{s}^{-1}$) and at night ($0.03 \mu\text{mol m}^{-2} \text{s}^{-1}$). The diurnal variation of the *S. japonica* farming period ranged from -0.23 – 0.26 (average of 0.02) $\mu\text{mol m}^{-2} \text{s}^{-1}$. The fluctuation of diurnal variation of NEE during the *S. japonica* farming period was smaller than that during the *G. Lemaneiformis* farming period. For *G. Lemaneiformis* farming, the ecosystem acted as a weaker daytime sink ($-0.11 \mu\text{mol m}^{-2} \text{s}^{-1}$) and a stronger nighttime source ($0.23 \mu\text{mol m}^{-2} \text{s}^{-1}$), ranging from -0.52 – $0.63 \mu\text{mol m}^{-2} \text{s}^{-1}$ with a daily mean flux of $0.06 \mu\text{mol m}^{-2} \text{s}^{-1}$. In contrast to these two farming periods, the non-farming period had much larger diurnal fluctuations in NEE, showing a stronger CO₂ source both during the daytime ($0.22 \mu\text{mol m}^{-2} \text{s}^{-1}$) and at night ($0.99 \mu\text{mol m}^{-2} \text{s}^{-1}$) (Fig. 5a). The daily mean NEE fluxes for the rapid growth, middle growth, and harvesting stages were $-0.27 \mu\text{mol m}^{-2} \text{s}^{-1}$, $0.20 \mu\text{mol m}^{-2} \text{s}^{-1}$ and $0.18 \mu\text{mol m}^{-2} \text{s}^{-1}$, respectively (Fig. 5b). At the rapid growth stage, the ecosystem acted as a strong CO₂ sink with larger contribution from nighttime sink ($-0.35 \mu\text{mol m}^{-2} \text{s}^{-1}$) than the daytime ($-0.18 \mu\text{mol m}^{-2} \text{s}^{-1}$). At the middle growth stage, the system acted as a source throughout the day (0.17 and $0.23 \mu\text{mol m}^{-2} \text{s}^{-1}$ for daytime and nighttime, respectively). At the harvesting stage, the

ecosystem was a weak CO₂ source during the daytime ($0.06 \mu\text{mol m}^{-2} \text{s}^{-1}$) but a strong source ($0.31 \mu\text{mol m}^{-2} \text{s}^{-1}$) at night.

3.4. Environmental controls on CO₂ flux

Pearson's correlation analyses were conducted to explore the links between daily NEE and related environment variables (Fig. 6). For all day, the NEE was statistically significantly ($p < 0.05$) correlated with radiation (0.24), WS (-0.15), Ta (0.41), Tw (0.21) and DO (-0.18). Since water quality factors were jointly affected by tidal activity (Fig. 6), we further examined the coupling relationship among NEE and major factors including Tw, DO, Chl-a, and tidal level based on their mean diurnal variations (Fig. 7). The temporal variability of these water quality factors tended to couple with the semi-diurnal tidal pattern, with overall opposite diurnal variations in Tw and DO from tidal water level. Mean diurnal variations of these variables indicated that tidal water level tended to peak around noon, and for most months peaking tidal level corresponded to an increase in NEE.

To further explore the tidal impacts on NEE, we divided flux and environmental data into "slow" and "fast" groups for both flood and ebb tides (Fig. 8). For wind speed and Ta whose fitting lines were statistically significant for both flood and ebb tides, faster tidal currents were found to exert positive effects on NEE (i.e., fitting lines are statistically

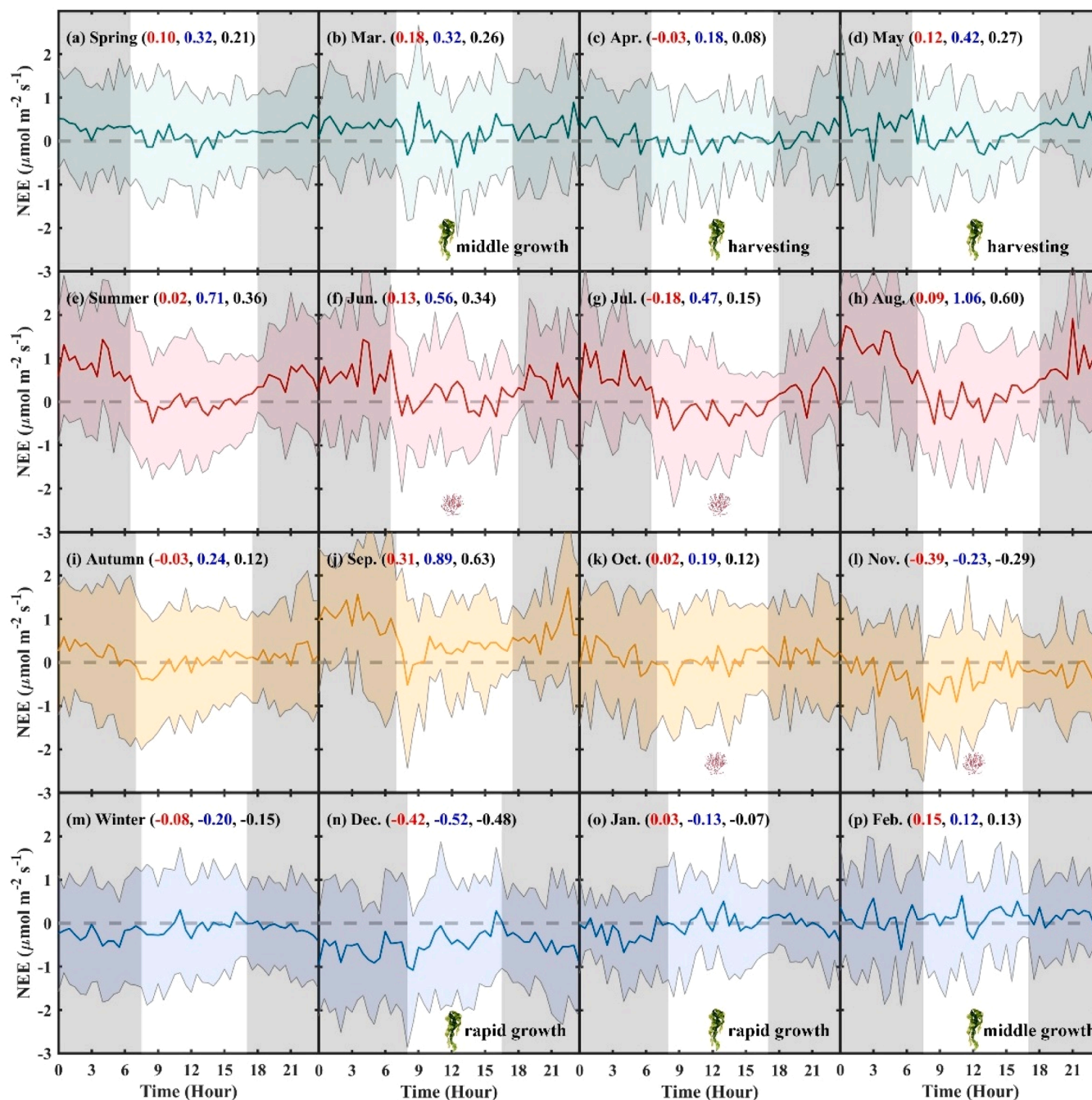


Fig. 4. Mean diurnal variations (MDV) and standard deviations in net ecosystem exchange (NEE) over the macroalgae aquaculture for each season and month from April 2023 to March 2024, with macroalgae farming months of *S. japonica* and *G. Lemaneiformis* labeled. Daytime and nighttime are indicated by white and gray areas, respectively. Mean flux values during the daytime (red), nighttime (blue), and throughout the day (black) based on each MDV are also shown.

different at $p < 0.05$) (Fig. 8a-d). For example, at the same T_a , the mean flux during flood tide was $0.22 \mu\text{mol m}^{-2} \text{s}^{-1}$ for faster tidal currents but only $0.08 \mu\text{mol m}^{-2} \text{s}^{-1}$ for slower tidal currents (Fig. 8c); during ebb tide, the mean flux at faster tidal currents reached $0.21 \mu\text{mol m}^{-2} \text{s}^{-1}$, while for slower tidal currents the mean flux only reached $0.03 \mu\text{mol m}^{-2} \text{s}^{-1}$ (Fig. 8d). Tidal impacts on NEE also differed between the flood and ebb, where the difference caused by faster and slower currents tended to be larger for the ebb than the flood. For example, under the same conditions of T_w and DO , the differences in NEE caused by tidal currents during the flood were only 0.10 and $0.07 \mu\text{mol m}^{-2} \text{s}^{-1}$, respectively (Figs. 8e and 8g), whereas such differences were 0.18 and $0.21 \mu\text{mol m}^{-2} \text{s}^{-1}$ during the ebb, respectively (Figs. 8f and 8h). Mean variations in NEE and wind speed across tidal levels (Fig. S3) indicated

that the NEE tended to be higher at faster tidal currents (i.e., 3 H and 4 H) and wind speeds.

4. Discussion

4.1. Net CO_2 flux in macroalgae aquaculture ecosystems

The study suggests that the macroalgae aquaculture area in Sansha Bay acts as a CO_2 source ($58.9 \text{ g C m}^{-2} \text{ year}^{-1}$), which is consistent with one previous study in the same bay ($0.01 \text{ g C m}^{-2} \text{ year}^{-1}$; Wei et al., 2016) but different from many other studies revealing that macroalgae aquaculture functions as a CO_2 sink ($-143.3 \sim -5.3 \text{ g C m}^{-2} \text{ year}^{-1}$; Jiang et al., 2013; Liu et al., 2017; Han et al., 2021b). Besides inherent

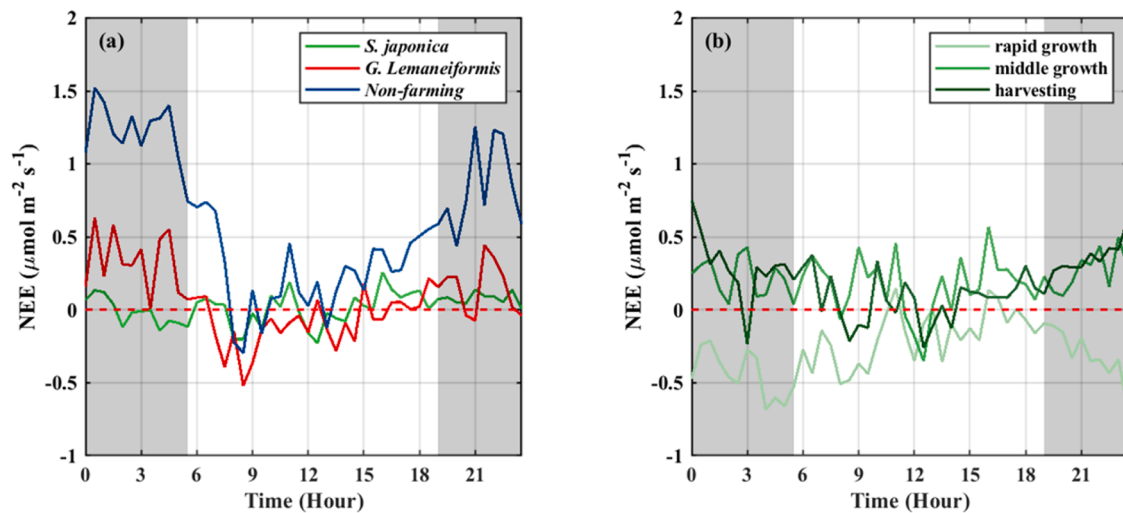


Fig. 5. Mean diurnal variations in net ecosystem exchange (NEE) over the (a) macroalgae aquaculture for different farming (*S. japonica* or *G. Lemaneiformis*) and non-farming periods and (b) growth stages of *S. japonica*. Daytime and nighttime are indicated by white and gray areas, respectively.

differences among in-situ environments, the magnitude of CO₂ source or sink estimated from various flux calculation methods could also vary greatly (Tokoro and Kuwae, 2018). For example, despite the same bay, our EC-based direct estimation of NEE (average of 0.12 $\mu\text{mol m}^{-2} \text{s}^{-1}$) is several orders of magnitude higher than that of the previous study (average of $2.93 \times 10^{-5} \mu\text{mol m}^{-2} \text{s}^{-1}$) based on the indirect bulk method (Wei et al., 2016). However, our EC-based NEE (average of 0.28 $\mu\text{mol m}^{-2} \text{s}^{-1}$) is comparable with the flux estimation (average of 0.73 $\mu\text{mol m}^{-2} \text{s}^{-1}$) based on the floating chamber method over a 72-hour observation period in March of 2024 (Fig. S4). The monthly diurnal variation of NEE shows that the farming area is a weak source of CO₂ during the day and a strong source of CO₂ at night for most of the time, which suggests that the macroalgae photosynthesis during the day might not fully offset the emission of CO₂. The difference between daytime and nighttime fluxes is not consistent throughout the year in this study, suggesting that the effect of diurnal variation on estimating carbon budgets should be assessed on a seasonal or even monthly basis.

Most previous studies focus on the diurnal variability of NEE based on discontinuous flux measurements with short measurement periods. In this study, NEE in macroalgae aquaculture shows a more pronounced seasonal variation, tending to function as a source of CO₂ in summer and a sink of CO₂ in winter (Fig. 4). The high temperature of surface seawater in summer decreases the solubility of CO₂ in seawater, which favors the emission of CO₂ into the atmosphere. Also, the absence of macroalgae aquaculture in summer due to the higher water temperature accounts for the occurrence of a stronger CO₂ source in summer. In winter, lower seawater surface temperatures result in lower partial pressures of CO₂ at the sea surface, and CO₂ is less likely to be emitted to the atmosphere. Meanwhile, the lower water temperature is suitable for the growth of macroalgae and can weaken the rates of respiration and mineralization of microorganisms to a certain extent (Feng et al., 2022; Sun et al., 2023). A study of CO₂ fluxes in a shellfish and macroalgae aquaculture area in Sanggou Bay of North China also indicated that autumn and winter were strong sinks of CO₂ (Liu et al., 2022). However, different from the macroalgae aquaculture in Sanggou Bay showing a more obvious carbon dioxide sink throughout the winter (Xiong et al., 2024), this study only shows an obvious carbon sink for one month in December. This difference could be attributed to the fact that the aquaculture area in temperate Sanggou Bay has lower winter air temperature than the aquaculture area in this subtropical bay. Active cage aquaculture of sea cucumber cultivation most occurring in winter could also affect the NEE since they're also covered by the EC footprint climatology (Fig. S1). However, our footprint analyses suggest that the

impact of sea cucumber cultivation on the NEE should be relatively small given there is no significant difference in mean diurnal variations of winter NEE between with and without considering the 30-min NEE most contributed by the sea cucumber cultivation (Fig. S5).

Although the region generally behaves as a source of CO₂, we cannot ignore the role of macroalgae aquaculture in weakening CO₂ emissions in the region. The average diurnal fluxes during *S. japonica* and *G. Lemaneiformis* farming periods are much smaller than the CO₂ fluxes during the non-farming period (Figs. 3 and 5). In this study, the ecosystem tends to shift from a CO₂ sink (December 2023 ~ January 2024 for rapid growth stage) to a CO₂ source (February ~ March 2024 and April ~ May 2023 for middle growth and harvesting stages, respectively) at different stages of the *S. japonica* farming period, which is similar to the findings of Xiong et al. (2024) that seawater changed from a CO₂ sink (lower $p\text{CO}_2$ by 17–73 μatm compared with the non-farming seawater) during the rapid growth period of kelp to a CO₂ source (higher $p\text{CO}_2$ by 20–37 μatm) during the aging period in Sanggou bay. The carbon content of kelp is found to decrease with the growth cycle and thus kelp contains more carbon as the juvenile than as the adult (Zhang et al., 2024), which could explain the apparent carbon sink observed during the rapid growth stage in this study. April and May are the harvesting periods for kelp, when more available biomass carbon accounts for the higher emission of CO₂ (Zhang et al., 2017; Xiong et al., 2023, 2024). It is reported that macroalgae may lose 8–61 % of their biomass due to fragmentation and erosion of fronds (Pessarrodona et al., 2024), and the rate of release of organic matter from kelp to seawater increases with the growth rate of kelp (Chen et al., 2020).

4.2. Environmental controls on net CO₂ flux

Coastal semi-enclosed bays are critical areas for biogeochemical reactions, and both anthropogenic activities and natural conditions such as tidal activity can impact water quality and CO₂ flux (Song et al., 2022; Fu et al., 2023). It is most likely that the weak source of CO₂ in this macroalgae aquaculture area during the day is related to CO₂ uptake by macroalgae photosynthesis and the strong source at night is related to the respiration of the ecosystem (Jiang et al., 2013; Ortega et al., 2019). In August and September of 2023 in the absence of macroalgae aquaculture, the area acts a strong nighttime but a weak daytime CO₂ source (Fig. 3a-b), which could be attributed to the contribution of phytoplankton as indicated by high Chl-a content (Fig. 2c). Consistent with previous studies (Li et al., 2022b), seawater DO in this bay is higher in spring and winter and lower in summer and autumn. Correlation

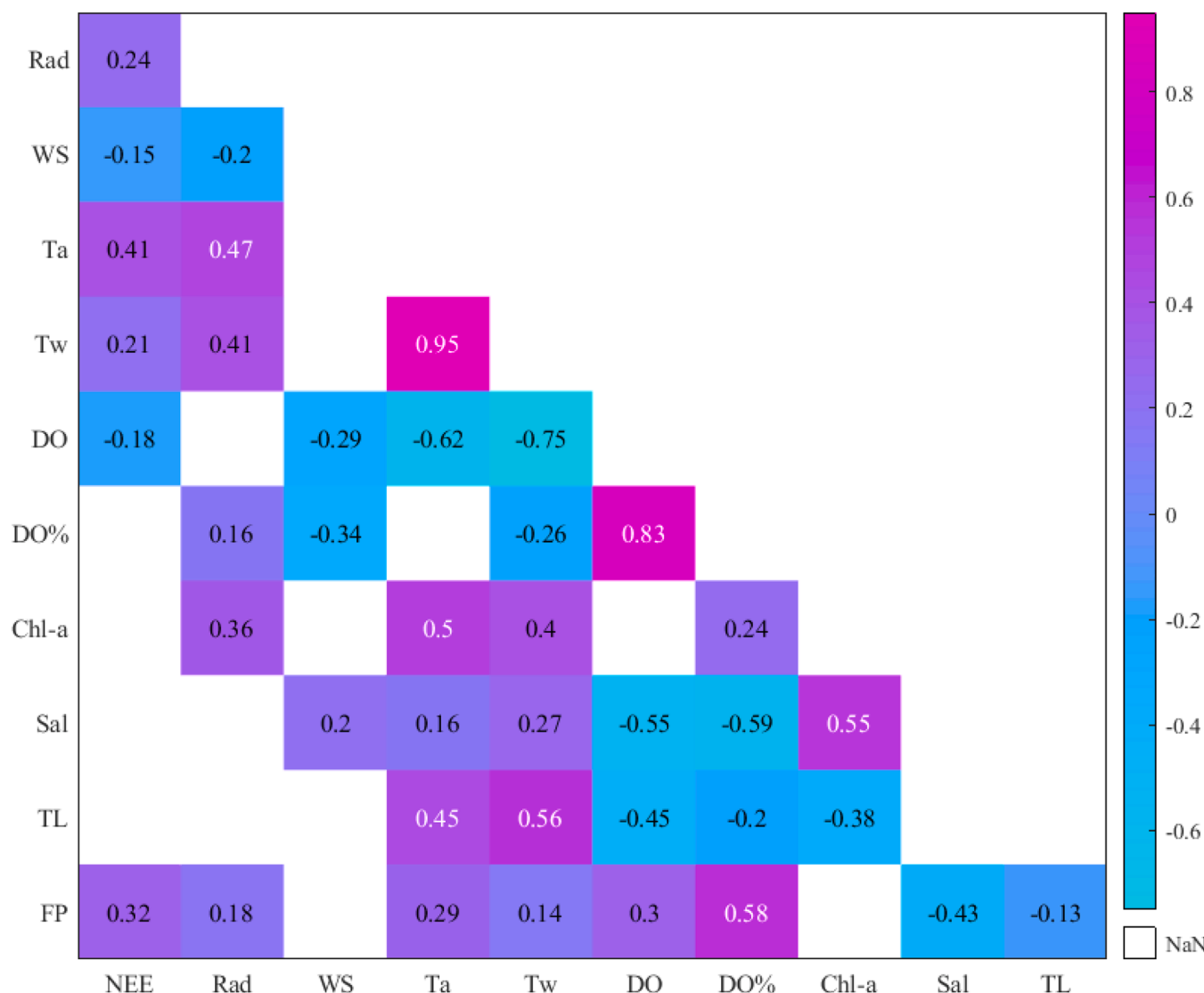


Fig. 6. Heatmaps of Pearson’s correlation coefficients between daily NEE and environmental factors, including radiation (Rad), wind speed (WS), air temperature (Ta), water temperature (Tw), dissolved oxygen (DO), percentage of dissolved oxygen (DO%), chlorophyll-a (Chl-a), tidal level (TL), and 90 % footprint (FP). The correlation coefficients were calculated on a pairwise basis to relieve the missing data issue. All shown coefficients are statistically significant at $p < 0.05$, while blank cells denote not significant (N.S.).

analyses also confirm a negative correlation between DO and NEE (Fig. 6), which is because photosynthesis increases the DO content when absorbing DIC, while respiration releases DIC and decreases the DO content in seawater (Vachon et al., 2020).

Besides the macroalgae aquaculture area itself, the NEE over the tidal bay ecosystem could be also affected by background seawater inflows from outside of the aquaculture area (e.g., higher CO₂ emissions via the inflow of seawater with higher pCO₂). This tidal disturbance might partially explain why the peaking tidal level around noon corresponds to an increase in NEE for most months (Fig. 7). However, given that the aquaculture area surrounding the EC tower is much larger than the EC footprint and there is no river running into the inner part of the bay where the EC tower is located, the effects of background seawater might be relatively small. Another possible reason contributing the temporal variability of NEE is the changing air-sea gas transfer velocity (e.g., a higher transfer velocity at stronger tidal currents and wind speeds) (Hahm et al., 2006; Fischereit et al., 2016), which might account for the positive effect of faster tidal currents on NEE (Fig. 8). In terms of the mean tidal variations in NEE and wind speed (Fig. S3), this bay ecosystem tends to emit more CO₂ at stronger tidal currents and wind

speeds, which also confirms the potential contribution of changing air-sea gas transfer velocity.

4.3. Limitations and implications

Field measurements and data analyses of this study suffer from several limitations and uncertainties. First, despite being able to capture the daily variation of NEE in aquaculture ecosystems with continuous and high-frequency measurements, EC-based CO₂ fluxes may be influenced by imperfect flux calibration and quality control processes. To decrease this uncertainty, we only analyze mean diurnal variations in NEE instead of individual days, which is statistically reasonable since 30-min NEE usually fluctuates significantly over any single day (Fig. S6) and thus it is almost impossible to accurately attribute the diurnal variability of NEE to any specific management activity within the day. Second, the EC-based NEE represents CO₂ fluxes over a spatial coverage (~400 m around the tower for the 90 % footprint climatology), but we are unable to accurately separate the contribution of NEE from the respective flux components, such as different macroalgae (*S. japonica* and *G. Lemaneiformis*). Third, although remote sensing imagery is

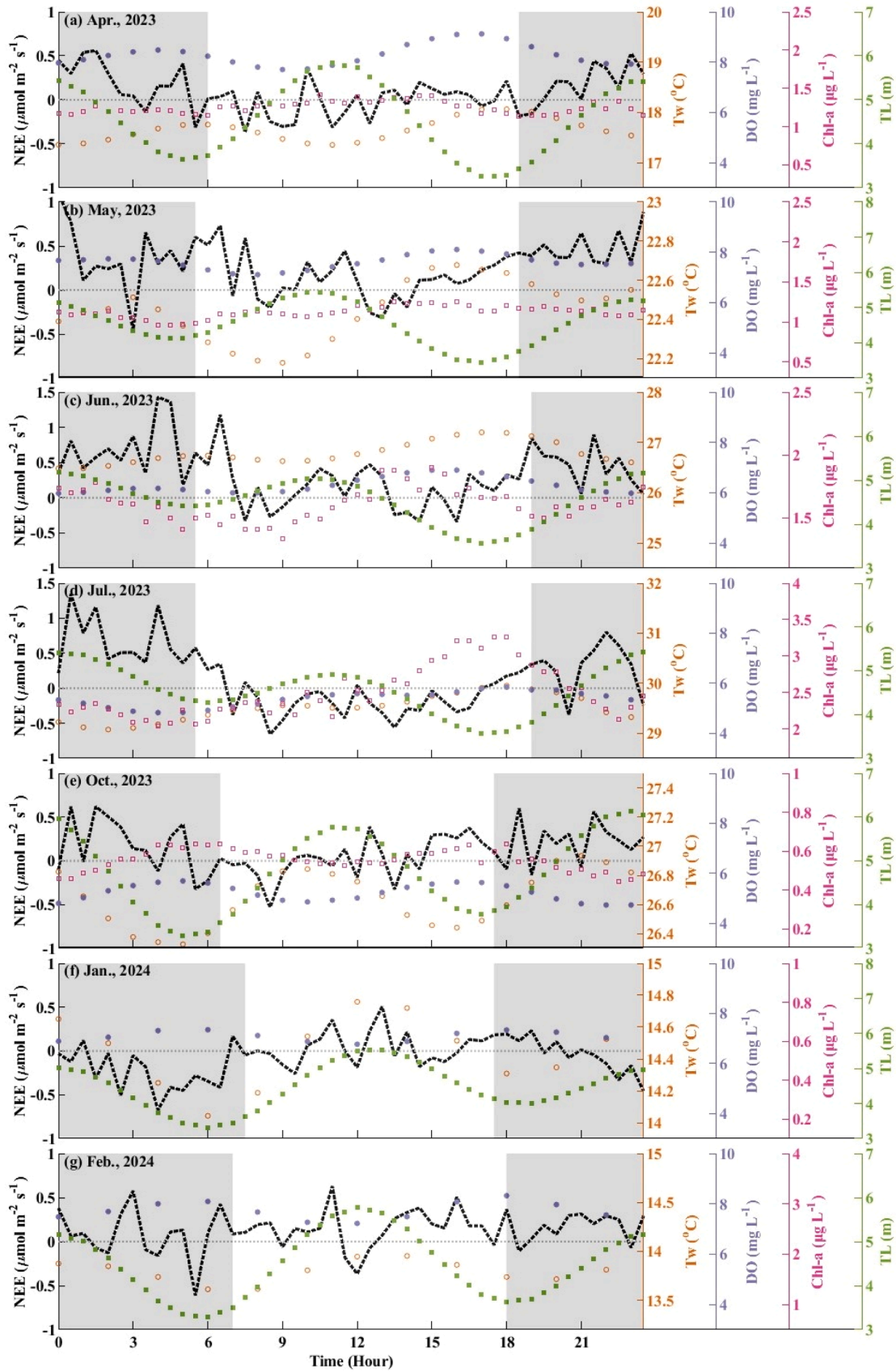
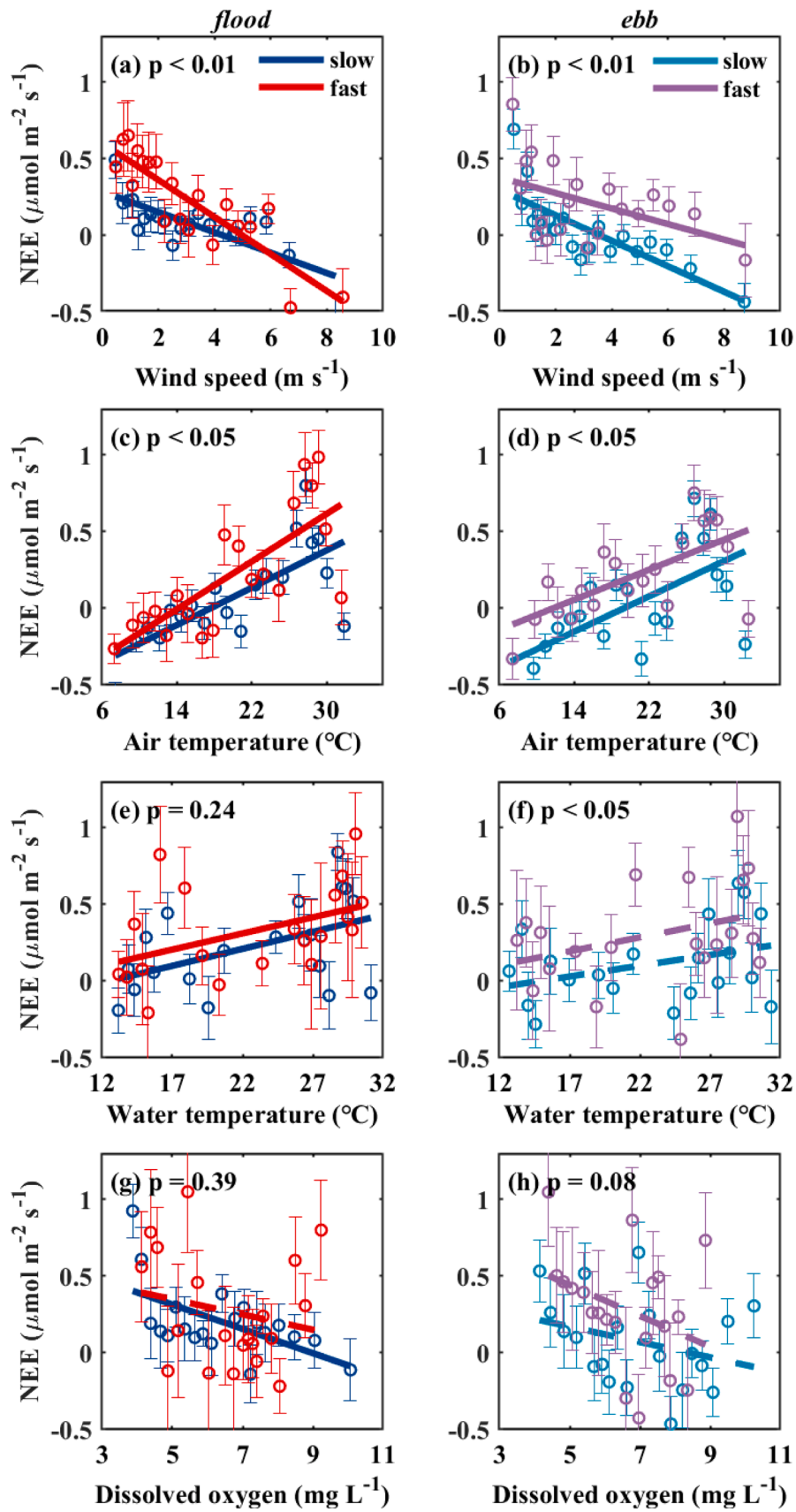


Fig. 7. Mean diurnal variations in net ecosystem exchange (NEE) over the macroalgae aquaculture and corresponding water quality factors, including water temperature (Tw), dissolved oxygen (DO), chlorophyll-a (Chl-a), and tidal level (TL), for seven months limited by data availability. Daytime and nighttime are indicated by white and gray areas, respectively.



(caption on next page)

Fig. 8. Tidal impacts on the responses of net ecosystem exchange (NEE) to major environmental factors including wind speed (a-b), air temperature (c-d), water temperature (e-f), and dissolved oxygen (g-h). The whole data were grouped by tidal level from low to high tide (1 H ~ 6 H) for both flood and ebb tides and then the “slow” and “fast” groups (Fig. S2) were binned by each environmental factor (20 percentile-based bins) to calculate the mean value and standard deviation. Linear regressions were applied to each group of data with solid and dashed lines indicating statistically significant ($p < 0.05$) and insignificant fittings, respectively. The p-value within each plot denotes the statistical significance of the difference between the “slow” and “fast” groups.

utilized in this study, there is some uncertainty in the temporal delineation of the macroalgae culture cycle because the mixing of different macroalgae types exists within a given month. Fourthly, temperature itself can exert a certain confounding effect on the temporal variability of CO₂ flux, since temperature affects seawater solubility and thus sea-air CO₂ exchange (Dai et al., 2009). Future studies should incorporate more field data such as simultaneous and continuous EC and pCO₂ measurements to disentangle the temperature-induced effect and better assess the contribution of macroalgae aquaculture itself.

In conclusion, the EC approach was applied in this study to acquire one full year of NEE measurements in a subtropical tide-driven enclosed bay in southeast China, aiming to better understand the temporal patterns of air-sea CO₂ fluxes and their environmental controls in macroalgae aquaculture ecosystems. The measured NEE shows strong temporal variations across diurnal, daily, and monthly time scales mainly driven by tidal and temperature fluctuations, which highlights the importance of high-frequency measurements to capture the temporal dynamics of NEE in such tide-driven bay ecosystems. As the first full-year EC study on macroalgae aquaculture, this study confirms that macroalgae aquaculture reduces CO₂ emissions particularly at its early rapid growth stage, although the ecosystem itself functions as a net CO₂ source on an annual time scale. Traditional approaches based on carbon stock changes or oxygen-based productivity measurements help identify the processes and factors in regulating NEE over macroalgae aquaculture ecosystems, but they fail to capture continuous and high-frequency fluctuations in NEE and thus may cause large uncertainties in developing informed climate mitigation strategies. Despite that the contribution of macroalgae aquaculture cannot be explicitly extracted using the EC approach, this study provides high-resolution measurements of direct air-sea CO₂ gas exchange, which is indispensable to determine whether the bay ecosystem with macroalgae aquaculture acts as a net source or sink of atmospheric CO₂ across various time scales and farming stages. Future studies should combine the EC approach with traditional ones to improve both temporal and process-oriented understanding of NEE fluctuations in macroalgae aquaculture, towards reducing uncertainties in estimating carbon budgets of this widely distributed but less-understood coastal ecosystem.

CRediT authorship contribution statement

Deng Yueting: Writing – original draft, Visualization, Investigation, Formal analysis, Data curation. **Guo Xianghui:** Writing – review & editing, Methodology, Investigation, Formal analysis. **Zhao Xiaosong:** Writing – review & editing, Methodology, Formal analysis, Conceptualization. **Zhou Haitao:** Visualization, Software, Formal analysis, Data curation. **Li Lichun:** Writing – review & editing, Software, Methodology, Formal analysis. **Chen Yougan:** Writing – review & editing, Visualization, Software, Conceptualization. **Zhu Xudong:** Writing – review & editing, Supervision, Project administration, Methodology, Investigation, Funding acquisition, Formal analysis, Data curation, Conceptualization.

Declaration of Competing Interest

The authors declare that they have no known competing financial interests or personal relationships that could have appeared to influence the work reported in this paper.

Acknowledgements

This work was jointly supported by the National Key Research and Development Program of China (2024YFF1306805, 2022YFF0802101), the National Natural Science Foundation of China (32371661), the Natural Science Foundation of Fujian Province of China (2023J06008), the Shenzhen Science and Technology Plan Project (KCXST20221021111404011), the Guiding Science & Technology Program of Fujian, China (2023N0029), the Open Fund of Fujian Key Laboratory of Severe Weather (2022KFKT03), and the 2023 Google Carbon Removal Research Awards. We are grateful to the staff at Zhangjiang Estuary Mangrove National Nature Reserve for their help in the fieldwork.

Appendix A. Supporting information

Supplementary data associated with this article can be found in the online version at [doi:10.1016/j.agee.2025.109576](https://doi.org/10.1016/j.agee.2025.109576).

Data availability

Data will be made available on request.

References

- Bach, L.T., Tamsitt, V., Gower, J., Hurd, C.L., Raven, J.A., Boyd, P.W., 2021. Testing the climate intervention potential of ocean afforestation using the Great Atlantic Sargassum Belt. *Nat. Commun.* 12, 2556. <https://doi.org/10.1038/s41467-021-22837-2>.
- Benson, B.B., Krause, D., 1984. The concentration and isotopic fractionation of oxygen dissolved in freshwater and seawater in equilibrium with the atmosphere. *Limnol. Oceanogr.* 29, 620–632. <https://doi.org/10.4319/lo.1984.29.3.0620>.
- Chen, S.W., Xu, K., Ji, D.H., Wang, W.L., Xu, Y., Chen, C.S., Xie, C.T., 2020. Release of dissolved and particulate organic matter by marine macroalgae and its biogeochemical implications. *Algal Res* 52, 102096. <https://doi.org/10.1016/j.algal.2020.102096>.
- Dai, M.H., Lu, Z.M., Zhai, W.D., Chen, B.S., Cao, Z.M., Zhou, K.B., Cai, W.J., Chen, C.T.A., 2009. Diurnal variations of surface seawater pCO₂ in contrasting coastal environments. *Limnol. Oceanogr.* 54, 735–745. <https://doi.org/10.4319/lo.2009.54.3.0735>.
- Duarte, C.M., 2017. Reviews and syntheses: Hidden forests, the role of vegetated coastal habitats in the ocean carbon budget. *Biogeosciences* 14, 301–310. <https://doi.org/10.5194/bg-14-301-2017>.
- Duarte, C.M., Bruhn, A., Krause-Jensen, D., 2022. A seaweed aquaculture imperative to meet global sustainability targets. *Nat. Sustain.* 5, 185–193. <https://doi.org/10.1038/s41893-021-00773-9>.
- Edson, J.B., Hinton, A.A., Prada, K.E., Hare, J.E., Fairall, C.W., 1998. Direct covariance flux estimates from mobile platforms at sea. *J. Atmos. Ocean. Technol.* 15, 547–562. [https://doi.org/10.1175/1520-0426\(1998\)015<0547:DCFEFM>2.0.CO;2](https://doi.org/10.1175/1520-0426(1998)015<0547:DCFEFM>2.0.CO;2).
- Feng, X.T., Li, H.M., Zhang, Z.H., Xiong, T.Q., Shi, X.Y., He, C., Shi, Q., Jiao, N.Z., Zhang, Y.Y., 2022. Microbial-mediated contribution of kelp detritus to different forms of oceanic carbon sequestration. *Ecol. Indic.* 142, 109186. <https://doi.org/10.1016/j.ecolind.2022.109186>.
- Filbee-Dexter, K., Pessarrodona, A., Duarte, C.M., Krause-Jensen, D., Hancke, K., Smale, D., Wernberg, T., 2023. Seaweed forests are carbon sinks that may help mitigate CO₂ emissions: a comment on Gallagher et al. (2022). *ICES J. Mar. Sci.* 80, 1814–1819. <https://doi.org/10.1093/icesjms/fsad107>.
- Fischereit, J., Schlünzen, K.H., Gierisch, A.M.U., Grawe, D., Petrik, R., 2016. Modelling tidal influence on sea breezes with models of different complexity. *Meteorol. Z.* 25, 343–355. <https://doi.org/10.1127/metz/2016/0703>.
- Fu, M.J., Lin, J.L., Zhang, P., Luo, W.S., Zhang, J.B., 2023. Tide drives nutrients variation and exchange flux in the semi-enclosed Shuidong Bay coastal water in winter, South China Sea. *Ocean Coast Manag* 242, 106710. <https://doi.org/10.1016/j.ocecoaman.2023.106710>.
- Gallagher, J.B., Shelamoff, V., Layton, C., 2022. Seaweed ecosystems may not mitigate CO₂ emissions. *ICES J. Mar. Sci.* 79, 585–592. <https://doi.org/10.1093/icesjms/fsac011>.
- Gao, G., Beardall, J., Jin, P., Gao, L., Xie, S.Y., Gao, K.S., 2022. A review of existing and potential blue carbon contributions to climate change mitigation in the

- Anthropocene. *J. Appl. Ecol.* 59, 1686–1699. <https://doi.org/10.1111/1365-2664.14173>.
- Hahm, D., Kim, G., Lee, Y.-W., Nam, S.-Y., Kim, K.-R., Kim, K., 2006. Tidal influence on the sea-to-air transfer of CH₄ in the coastal ocean. *Tellus B* 58. <https://doi.org/10.3402/tellusb.v58i1.16796>.
- Han, A.Q., Kao, S.-J., Lin, W.F., Lin, Q.Y., Han, L.L., Zou, W.B., Tan, E.H., Lai, Y., Ding, G. M., Lin, H., 2021a. Nutrient Budget and Biogeochemical Dynamics in Sansha Bay, China: A Coastal Bay Affected by Intensive Mariculture. *J. Geophys. Res. Biogeosci.* 126, e2020JG006220. <https://doi.org/10.1029/2020JG006220>.
- Han, T.Y., Shi, R.J., Qi, Z.H., Huang, H.H., Gong, X.Y., 2021b. Impacts of large-scale aquaculture activities on the seawater carbonate system and air-sea CO₂ flux in a subtropical mariculture bay, southern China. *Aquac. Environ. Interact.* 13, 199–210. <https://doi.org/10.3354/aei00400>.
- Hurd, C.L., Law, C.S., Bach, L.T., Britton, D., Hovenden, M., Paine, E.R., Raven, J.A., Tamsitt, V., Boyd, P.W., 2022. Forensic carbon accounting: Assessing the role of seaweeds for carbon sequestration. *J. Phycol.* 58, 347–363. <https://doi.org/10.1111/jpy.13249>.
- Hurd, C.L., Gattuso, J.P., Boyd, P.W., 2024. Air-sea carbon dioxide equilibrium: Will it be possible to use seaweeds for carbon removal offsets? *J. Phycol.* 60, 4–14. <https://doi.org/10.1111/jpy.13405>.
- Ikawa, H., Oechel, W.C., 2015. Temporal variations in air-sea CO₂ exchange near large kelp beds near San Diego, California. *J. Geophys. Res. Oceans* 120, 50–63. <https://doi.org/10.1002/2014JC010229>.
- Jiang, Z.J., Fang, J.G., Mao, Y.Z., Han, T.T., Wang, G.H., 2013. Influence of seaweed aquaculture on marine inorganic carbon dynamics and sea-air CO₂ flux. *J. World Aquacult. Soc.* 44, 133–140. <https://doi.org/10.1111/jwas.12000>.
- Kormann, R., Meixner, F.X., 2001. An analytical footprint model for non-neutral stratification. *Bound. Layer. Meteorol.* 99, 207–224. <https://doi.org/10.1023/A:1018991015119>.
- Krause-Jensen, D., Duarte, C.M., 2016. Substantial role of macroalgae in marine carbon sequestration. *Nat. Geosci.* 9, 737–742. <https://doi.org/10.1038/ngeo2790>.
- Li, H., Moon, H., Kang, E.J., Kim, J.-M., Kim, M., Lee, K., Kwak, C.-W., Kim, H., Kim, I.-N., Park, K.Y., Lee, Y.K., Jin, J.W., Edwards, M.S., Kim, J.H., 2022b. The diel and seasonal heterogeneity of carbonate chemistry and dissolved oxygen in three types of macroalgal habitats. *Front. Mar. Sci.* 9, 857153. <https://doi.org/10.3389/fmars.2022.857153>.
- Li, H.M., Zhang, Z.H., Xiong, T.Q., Tang, K.X., He, C., Shi, Q., Jiao, N.Z., Zhang, Y.Y., 2022a. Carbon sequestration in the form of recalcitrant dissolved organic carbon in a seaweed (kelp) farming environment. *Environ. Sci. Technol.* 56, 9112–9122. <https://doi.org/10.1021/acs.est.2c01535>.
- Liu, Y., Zhang, J.H., Fang, J.H., Lin, F., Wu, W.G., 2017. Analysis of the air-sea surface carbon dioxide flux and its interaction with aquaculture activities in Sanggou Bay. *Prog. Fish. Sci.* 38 (6), 1–8. <https://doi.org/10.11758/yykxjz.20160331001>.
- Liu, Y., Zhang, J.H., Wu, W.G., Zhong, Y., Li, H.M., Wang, X.M., Yang, J., Zhang, Y.Y., 2022. Effects of shellfish and macro-algae IMTA in north CHINA on the environment, inorganic carbon system, organic carbon system, and sea-air CO₂ fluxes. *Front. Mar. Sci.* 9, 864306. <https://doi.org/10.3389/fmars.2022.864306>.
- Mauder, M., Cuntz, M., Dri e, C., Graf, A., Rebmann, C., Schmid, H.P., Schmidt, M., Steinbrecher, R., 2013. A strategy for quality and uncertainty assessment of long-term eddy-covariance measurements. *Agric. For. Meteorol.* 169, 122–135. <https://doi.org/10.1016/j.agrformet.2012.09.006>.
- Ortega, A., Gheraldi, N.R., Alam, I., Kamau, A.A., Acinas, S.G., Logares, R., Gasol, J.M., Massana, R., Krause-Jensen, D., Duarte, C.M., 2019. Important contribution of macroalgae to oceanic carbon sequestration. *Nat. Geosci.* 12, 748–754. <https://doi.org/10.1038/s41561-019-0421-8>.
- Pan, Z., Gao, Q.F., Dong, S.L., Wang, F., Li, H.D., Zhao, K., Jiang, X.Y., 2019. Effects of abalone (*Haliotis discus hannai* Iino) and kelp (*Saccharina japonica*) mariculture on sources, distribution, and preservation of sedimentary organic carbon in Ailian Bay, China: Identified by coupling stable isotopes ($\delta^{13}C$ and $\delta^{15}N$) with C/N ratio analyses. *Mar. Pollut. Bull.* 141, 387–397. <https://doi.org/10.1016/j.marpolbul.2019.02.053>.
- Perkins, A.K., Santos, I.R., Rose, A.L., Schulz, K.G., Grossart, H.P., Eyre, B.D., Kelaher, B. P., Oakes, J.M., 2022. Production of dissolved carbon and alkalinity during macroalgal wrack degradation on beaches: a mesocosm experiment with implications for blue carbon. *Biogeochemistry* 160, 159–175. <https://doi.org/10.1007/s10533-022-00946-4>.
- Pessarrodona, A., Howard, J., Pidgeon, E., Wernberg, T., Filbee-Dexter, K., 2024. Carbon removal and climate change mitigation by seaweed farming: A state of knowledge review. *Sci. Total Environ.* 918, 170525. <https://doi.org/10.1016/j.scitotenv.2024.170525>.
- Ross, F.W.R., Boyd, P.W., Filbee-Dexter, K., Watanabe, K., Ortega, A., Krause-Jensen, D., Lovelock, C., Sondak, C.F.A., Bach, L.T., Duarte, C.M., Serrano, O., Beardall, J., Tarbuck, P., Macreadie, P.I., 2023. Potential role of seaweeds in climate change mitigation. *Sci. Total Environ.* 885, 163699. <https://doi.org/10.1016/j.scitotenv.2023.163699>.
- Roth, F., Broman, E., Sun, X.L., Bonaglia, S., Nascimento, F., Prytherch, J., Br uchert, V., Lundevall Zara, M., Brunberg, M., Geibel, M.C., Humborg, C., Norkko, A., 2023. Methane emissions offset atmospheric carbon dioxide uptake in coastal macroalgae, mixed vegetation and sediment ecosystems. *Nat. Commun.* 14, 1–11. <https://doi.org/10.1038/s41467-022-35673-9>.
- Song, S.Z., Gao, L., Ge, J.Z., Guo, W.Y., Li, D.J., 2022. Tidal effects on variations in organic and inorganic biogeochemical components in Changjiang (Yangtze River) Estuary and the adjacent East China Sea. *J. Mar. Syst.* 227, 103692. <https://doi.org/10.1016/j.jmarsys.2021.103692>.
- Sun, Y., Li, H.J., Wang, X.C., Li, H.B., Deng, Y., 2023. Kelp culture enhances coastal biogeochemical cycles by maintaining bacterioplankton richness and regulating its interactions. *mSystems* 8, e00002-23. <https://doi.org/10.1128/mSystems.00002-23>.
- Tokoro, T., Kuwae, T., 2018. Improved post-processing of eddy-covariance data to quantify atmosphere-aquatic ecosystem CO₂ exchanges. *Front. Mar. Sci.* 5. <https://doi.org/10.3389/fmars.2018.00286>.
- Vachon, D., Sadro, S., Bogard, M.J., Lapierre, J.F., Baulch, H.M., Rusak, J.A., Denfeld, B. A., Laas, A., Klaus, M., Karlsson, J., Weyhenmeyer, G.A., del Giorgio, P.A., 2020. Paired O₂-CO₂ measurements provide emergent insights into aquatic ecosystem function. *Limnol. Oceanogr. Lett.* 5, 287–294. <https://doi.org/10.1002/lo.12135>.
- Wada, S., Aoki, M.N., Mikami, A., Komatsu, T., Tsuchiya, Y., Sato, T., Shinagawa, H., Hama, T., 2008. Bioavailability of macroalgal dissolved organic matter in seawater. *Mar. Ecol. -Prog. Ser.* 370, 33–44. <https://doi.org/10.3354/meps07645>.
- Wang, Y.G., Song, Z.Y., Jiang, C.L., 2009. Numerical modeling and environmental study of gulf in FUJIAN province: Sansha Bay. China Ocean Press, Beijing.
- Watanabe, K., Yoshida, G., Hori, M., Umezawa, Y., Moki, H., Kuwae, T., 2020. Macroalgal metabolism and lateral carbon flows can create significant carbon sinks. *Biogeosciences* 17, 2425–2440. <https://doi.org/10.5194/bg-17-2425-2020>.
- Wei, Z.L., Han, H.B., Hu, M., Wu, H.L., Zhang, J.H., Huo, Y.Z., He, P.M., 2016. Seasonal variation of sea-air CO₂ flux in mariculture area in Yantian Harbor, Sansha Bay. *J. Shanghai Ocean Univ.* 25, 106–115. <https://doi.org/10.12024/jso.20150101314>.
- Weigel, B.L., Miranda, K.K., Fogarty, E.C., Watson, A.R., Pfister, C.A., 2022. Functional insights into the kelp microbiome from metagenome-assembled genomes. *mSystems* 7, e0142221. <https://doi.org/10.1128/mSystems.01422-21>.
- Xiong, T.Q., Li, H.M., Yue, Y.F., Hu, Y.B., Zhai, W.D., Xue, L., Jiao, N.Z., Zhang, Y.Y., 2023. Legacy effects of late macroalgal blooms on dissolved inorganic carbon pool through alkalinity enhancement in coastal ocean. *Environ. Sci. Technol.* 57, 2186–2196. <https://doi.org/10.1021/acs.est.2c09261>.
- Xiong, T.Q., Li, H.M., Hu, Y.B., Zhai, W.D., Zhang, Z., Liu, Y., Zhang, J.H., Lu, L.F., Chang, L.R., Xue, L., Wei, Q.S., Jiao, N.Z., Zhang, Y.Y., 2024. Seaweed farming environments do not always function as CO₂ sink under synergistic influence of macroalgae and microorganisms. *Agric. Ecosyst. Environ.* 361, 108824. <https://doi.org/10.1016/j.agee.2023.108824>.
- Ye, H.T., Wang, Y.G., Cao, B., 2007. Tidal prism of Sansha Bay and its water change with the open sea. *J. Hohai Univ.* 35 (1), 96–98.
- Zhang, Y.Y., Zhang, J.H., Liang, Y.T., Li, H.M., Li, G., Chen, X., Zhao, P., Jiang, Z.J., Zou, D.H., Liu, X.Y., Liu, J.H., 2017. Carbon sequestration processes and mechanisms in coastal mariculture environments in China. *Sci. China Earth Sci.* 60, 2097–2107. <https://doi.org/10.1007/s11430-017-9148-7>.
- Zhang, Z., Lei, L.Y., Wang, F.P., Li, R.M., Li, C., Huang, Y.L., Mu, J.L., 2024. Assessment and spatial pattern of carbon sequestration potential of mariculture in Sansha Bay. *Ocean Dev. Manag.* 41, 28–37. <https://doi.org/10.20016/j.cnki.hykyfjgl.20240019.003>.
- Zhu, X.D., Ma, M.H., Li, L.C., Li, M.J., 2024b. Impacts of intensive smooth cordgrass removal on net ecosystem exchange in a saltmarsh-mangrove ecotone of southeast China. *Sci. Total Environ.* 934, 173202. <https://doi.org/10.1016/j.scitotenv.2024.173202>.
- Zhu, X.D., Chen, J.K., Li, L.C., Li, M.J., Li, T.T., Qin, Z.C., Wang, F., Zhao, X.S., 2024a. Asynchronous methane and carbon dioxide fluxes drive temporal variability of mangrove blue carbon sequestration. *Geophys. Res. Lett.* 51, e2023GL107235. <https://doi.org/10.1029/2023GL107235>.
- Zhu, X.D., Sun, C.Y., Qin, Z.C., 2021. Drought-induced salinity enhancement weakens mangrove greenhouse gas cycling. *J. Geophys. Res. Biogeosci.* 126 (8), e2021JG006416. <https://doi.org/10.1029/2021JG006416>.